# ANGULAR DEPENDENCE OF THE RESONANT MAGNETOSTATIC FIELD FOR PLANAR FERRITES

by

Merrill A. Green, Jr.

---

A Thesis Submitted to the Faculty of the

DEPARTMENT OF ELECTRICAL ENGINEERING

In Partial Fulfillment of the Requirements
For the Degree of

MASTER OF SCIENCE

In the Graduate College

THE UNIVERSITY OF ARIZONA

1 9 6 4

STATEMENT BY AUTHOR

This thesis has been submitted in partial fulfillment of requirements for an advanced degree at The University of Arizona and is deposited in the University Library to be made available to borrowers under rules of the Library.

Brief quotations from this thesis are allowable without special permission, provided that accurate acknowledgment of source is made. Requests for permission for extended quotation from or reproduction of this manuscript in whole or in part may be granted by the head of the major department or the Dean of the Graduate College when in his judgment the proposed use of the material is in the interests of scholarship. In all other instances, however, permission must be obtained from the author.

SIGNED: Merrill A. Green Jr

APPROVAL BY THESIS DIRECTOR

This thesis has been approved on the date shown below:

Donald C. Stinson

DONALD C. STINSON
Professor of Electrical Engineering

May 5, 1964
Date

ACKNOWLEDGMENT

The author wishes to express his appreciation to Dr. Donald C. Stinson for his counsel, instruction, and patient understanding without which this thesis would never have been completed

TABLE OF CONTENTS

LIST OF FIGURES

ABSTRACT

The resonant magnetostatic field and line width of two different single crystal planar ferrites ($Zn_2Y$ and $Mn_{0.5}Zn_{1.5}Y$) were measured as a function of the angular orientation of the magnetic microwave field and the basal plane of the crystal. These measurements were made at X-band.

The angular dependence of the resonant magnetostatic field was different for the two ferrites. For $Mn_{0.5}Zn_{1.5}Y$ the resonant field was independent of angle as predicted by the basic resonance equation. For $Zn_2Y$ the angular dependence produced an irregular curve that had a minimum and maximum with $h_{rf}$ parallel and $h_{rf}$ perpendicular to the basal plane respectively. This behavior is attributed to anisotropic g factors.

Using a zero degree angle reference of $h_{rf}$ parallel to the basal plane, the angular dependence of line width for both compounds was a sine squared of the angle. An exception to this behavior existed with $Zn_2Y$. A line width reversal occurred with this compound at 8.7gc and is explained by the existence of anisotropic g factors.

Frequency behavior of the resonant magnetostatic field and line width for both compounds was in agreement with the existing theories. The experimental results were

used to compute pertinent constants of the two ferrites and the results of these computations were in excellent agreement with other sources.

# CHAPTER I

# INTRODUCTION

## 1.1 General Background

In 1909 Hilpert identified the basic formula for simple ferrites, $MeO \cdot Fe_2O_3$. In this formula, Me can represent any divalent metal ion. $Fe_3O_4$, however, is the only simple ferrite found in nature. Hilpert's investigation of these compounds was motivated by the shortcomings of existing transformer cores. He prepared several simple ferrites and secured patents on some of them as transformer cores. However, his ferrites could not be reliably reproduced and still exhibited the undesirable losses and low permeabilities at increased frequencies. Laminated sheets and powdered iron cores were developed about this time and the practical investigation of ferrites was no longer of prime interest (1).

During the next two decades, fundamental and practical research on ferrites was essentially non-existent. However, the advent of the 1930's saw a renewed search into the use of ferrites. From 1933 until the end of World War II, the bulk of ferrite research and development was performed at the Philips Research Laboratory at Eindhoven, Holland. It was here that ferrites acquired commercial

significance. Snoek and his co-workers are credited with the bulk of this work (1).

After World War II fundamental research on the theory of magnetism was renewed. Verwey and Heilman (1) made x-ray diffraction studies in 1947 on some oxides that have a spinel crystal structure to determine their different lattice constants. Their experimental findings and those of many others could not be explained by the existing theory of magnetism. However, in 1948 Neel (2) announced his theory of magnetism which could explain his contemporaries' experimental findings. His theory basically postulated that the spin-spin interaction taking place in magnetic oxides and antiferromagnetic materials was a negative super-exchange interaction. This exchange interaction is similar to that observed in ferromagnetic materials except that the electron spins will orient, via an intermediary, in an antiparallel sense. Neel called this antiparallel alignment of spins ferrimagnetism in contrast to the parallel alignment of spins in ferromagnetism. Hereafter, no distinction between the two cases will be made in this paper.

Neel's theory was to provide a secure building block for the extensive magnetism research in the years to come. Anderson and Van Vleck supplemented the theory with a detailed quantum-mechancial evaluation of all the possible electron spin interactions. It was not until 1951

that any direct proof of Neel's theory was to be observed. Shull utilized neutron diffraction techniques rather than x-ray diffraction and was able to observe the anti-ferromagnetic alignment of $Fe_3^+$ ions in magnetite (1).

The Dutch announced the barium "ferrites" in the early 1950's. These compounds do not fit the simple formula as given by Hilpert, but are commonly called ferrites as are the ferrimagnetic garnets. The barium "ferrites" are the only ferrimagnetic oxides to be considered in this thesis; therefore, the word ferrite will be used in referring to these compounds. These hexagonal crystal ferrites have acquired current interest and importance as they were found to have the large magnetocrystalline anisotropy fields desirable for some microwave applications (3). The orientation of these anisotropy fields can be either uniaxial or planar depending on the specific compound (4) These barium ferrites, specifically the planar variety, will be considered in more detail in Chapter II.

## 1.2 Statement of the Problem

To use any ferrite practically, its properties and behaviors should be known and understood. The purpose of this thesis is to investigate the angular dependence of the resonant magnetostatic field and the line width for two planar ferrites at X-band frequencies.

## 1.3 Method of Treatment

Spherical samples of each planar ferrite will be placed individually in a modified crossguide coupler. Angular rotation of the sample will be made without the disturbance of any other parameters in the system. Each ferrite will be oriented on a mounting rod so that the axis of rotation is parallel to the basal plane. The basal plane is defined as the hexagonal plane of crystal symmetry and is often called the "easy" plane for the planar ferrites.

A magnetostatic field sufficient for resonance will be applied parallel to this axis of rotation. Figure 1.1 gives a pictorial description of the crystal orientation and coordinate system selected and utilized throughout this thesis. The hexagon in the diagram represents the crystal's basal plane and will be fixed in the X-Y plane. Analogous sample rotation is performed by having the magnetic microwave field rotate in the X-Z plane around the Y axis. Aside from the ease of illustrating a hexagon, this is done to be consistent with a later diagram used in the derivation of the basic resonance equation.

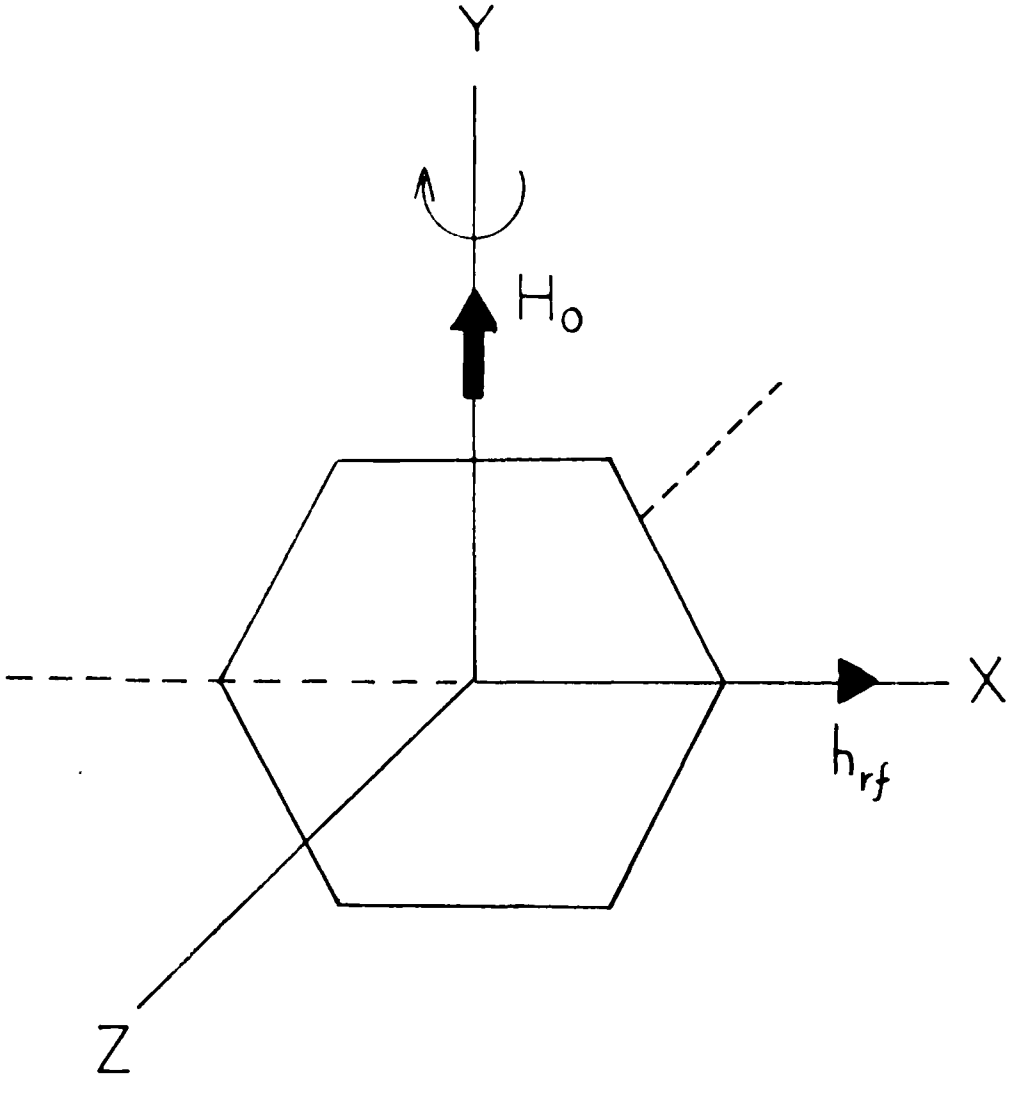


Figure 1.1 Crystal Orientation and Coordinate System

# CHAPTER II

# THEORY

## 2.1 Physical Characteristics

Figure 2.1 is a chemical composition triangle (4) that is useful in understanding the chemical composition and interrelation of the various barium ferrites. The different letter designations on the diagram were initiated by the Dutch and are in common usage today. The right side of this triangle represents the true ferrites with point S designating the ferrite spinels. The other lettered points represent specific barium ferrites that have been reliably reproduced and that are of commercial interest. At this time, M and Y compounds have had significant commercial use to have tradenames of Ferroxdure and Ferroxplana, respectively. W and Z compounds have no present commercial use but represent the most reliably produced mixed compounds.

The crystal structure of the barium ferrites is quite complicated; however, they all exhibit the hexagonal crystal symmetry. The exact crystal structure and composition will determine the magnitude and orientation of electron spins. In most all of the compounds, except Y compounds, the preferred direction of electron spin alignment is normal to the basal plane. This preferred

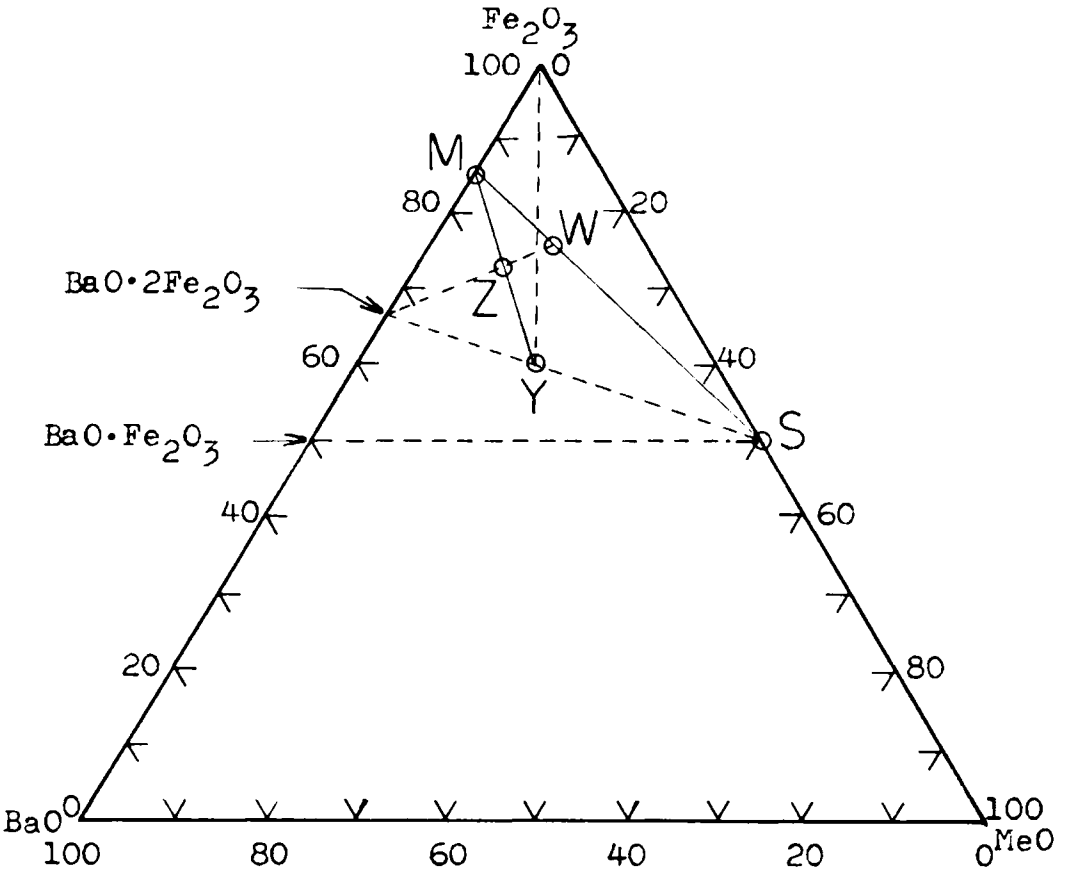


$S = MeO \cdot Fe_2O_3$

$M = BaO \cdot 6Fe_2O_3$

$W = BaO \cdot 2MeO \cdot 8Fe_2O_3$

$Y = 2BaO \cdot 2MeO \cdot 6Fe_2O_3$

$Z = 3BaO \cdot 2MeO \cdot 12Fe_2O_3$

Figure 2.1 Chemical Composition Triangle for Barium Ferrites

direction is usually called the C axis, easy axis, or hexagonal axis and is represented in Figure 1.1 by the Z axis. For Y compounds and any other compound with cobalt, the preferred orientation of electron spins is in the basal plane wherein it is relatively free to rotate (4). For this thesis, only the Y compounds will be discussed. The raw crystals of two planar ferrites have been kindly supplied by Mr. A. Tauber of the Institute of Exploratory Research, USAERDL, Fort Monmouth, N.J.

The general Y compound formula is $2BaO \cdot 2MeO \cdot 6Fe_2O_3$. A shorthand notation of $Me_2Y$ is often used for simplicity. The subscript of the Me in this notation is identical with the proportion constant prefixing the MeO in the general chemical formula. The two planar ferrites supplied by Tauber can now be designated as $Zn_2Y$ and $Mn_{0.5}Zn_{1.5}Y$.

The crystal structure of Y compounds was determined by Braun (4). Although crystallography will not be considered in this paper, a simplified explanation for the electron spins aligning in the basal plane will be made. Basically, the Y compounds are formed of alternate predominately barium or oxygen layers with the divalent metal ions occupying the available sites within these stratified layers. One cation (divalent metal ion) of the barium layer occupies an available site such that its negative super exchange interaction becomes the dominate influence for spin alignment. This results in the planar

alignment of spins within the barium layer and ultimately within the entire crystal (1). Any further discussion of a microscopic nature is not necessary for understanding their microscopic behavior. Fortunately, the net alignment of spins in these compounds can be considered as a resultant magnetization vector. This permits the concept of magnetocrystalline anisotropy fields to be introduced (4). These anisotropy fields are defined as the magnetostatic field required to rotate the magnetization vector from its most preferred direction to its least preferred direction. In planar ferrites, these fields are usually denoted by $H_\theta$ and $H_\phi$. The subscripts indicate the standard angles used in spherical coordinates. $H_\theta$ then, is that magnetostatic field required to align the magnetization vector with the hexagonal axis (Z axis, Figure 1.1) and $H_\phi$ is that magnetostatic field required to rotate the magnetization vector in the basal plane (XY plane, Figure 1.1). The difference in magnitude of these two fields is very large. For $Zn_2Y$, $H_\theta$ is 9000 to 9900 oersteds while $H_\phi$ is less than one oersted (4, 5). Data on $Mn_{0.5}Zn_{1.5}Y$ is not available. However, information supplied by Tauber (6) indicate that $H_\theta$ should be no less than 90 percent of the $H_\theta$ for $Zn_2Y$. $H_\phi$ will be less than one oersted.

## 2.2 Derivation of Resonance Equation

Classically the gyromagnetic properties of ferrites result from the precession of electron spins around a magnetization vector produced by an externally applied magnetostatic field. The general equation of motion in such a system is (7):

$$\frac{1}{\gamma}\frac{d\vec{M}}{dt} = \vec{M} \times \vec{H}_t \qquad (1)$$

where: $\gamma$ = magnetomechanical ratio

$\vec{M}$ = magnetization of the medium

$\vec{H}_t$ = total internal magnetic field of the medium

CGS, "Gaussian," units will be used in this thesis as is the common practice in the ferrite literature. In (1) then, $\gamma = \frac{g|e|}{2mc}$ with g representing the apparent g factor; e and m representing the electron charge and mass, respectively; and c representing the speed of light. The unit of $\gamma$ is radians per sec per gauss. The units of $\vec{M}$ and $\vec{H}_t$ are gauss and oersteds, respectively. An appropriate conversion factor will be applied later to $\gamma$ such that the resonance equation can be expressed in terms of frequency rather than angular frequency.

The effect of any anisotropy field can be introduced into (1) by an additional torque, $\vec{T}_a$ (8). The effect due to anisotropic magnetocrystalline energy is introduced in this manner. However, before the desired solution of the resulting equation of motion is possible, the

anisotropy torque must first be expressed in terms of the magnetization vector ($\vec{M}$) and the anisotropy field ($H_a$). A pictorial representation of the anisotropy torque and magnetization vectors is given in Figure 2.2. To arrive at the special case in this thesis, $\vec{T}_a$ is considered as being in the X-Y plane with $\vec{M}$ being arbitrarily oriented and having the conventional direction cosines ($\alpha$, $\beta$, $\gamma$). These direction cosines are not shown in Figure 2.2 for reasons of clarity.

Smit and Wijn (4) have shown that the magnetocrystalline anisotropy energy can be expressed as the first two terms of the infinite power series in the magnetization vector's direction cosines. The resulting expression for the energy of materials with one axis of symmetry is given in spherical coordinates as (4):

$$E_a = K_1 \sin^2\theta + K_2 \sin^4\theta + \ldots \qquad (2)$$

The torque due to this energy is defined to be (8):

$$\vec{T}_a = -\frac{\partial E_a}{\partial \theta}\,\vec{a}_t \qquad (3)$$

$$\vec{T}_a = -2(K_1 \sin\theta\cos\theta + 2K_2 \sin^3\theta\cos\theta)\,\vec{a}_t$$

where: $\vec{a}_t$ is a unit vector determined by crossing $\vec{a}_z$ into $\vec{M}$.

For the case where $\theta \approx \frac{\pi}{2}$ and $|\vec{M}| = M_s$, simplifying assumptions of $\sin\theta \approx 1$ and $\cos\theta \approx \frac{M_z}{M_s}$ reduce the torque expression to:

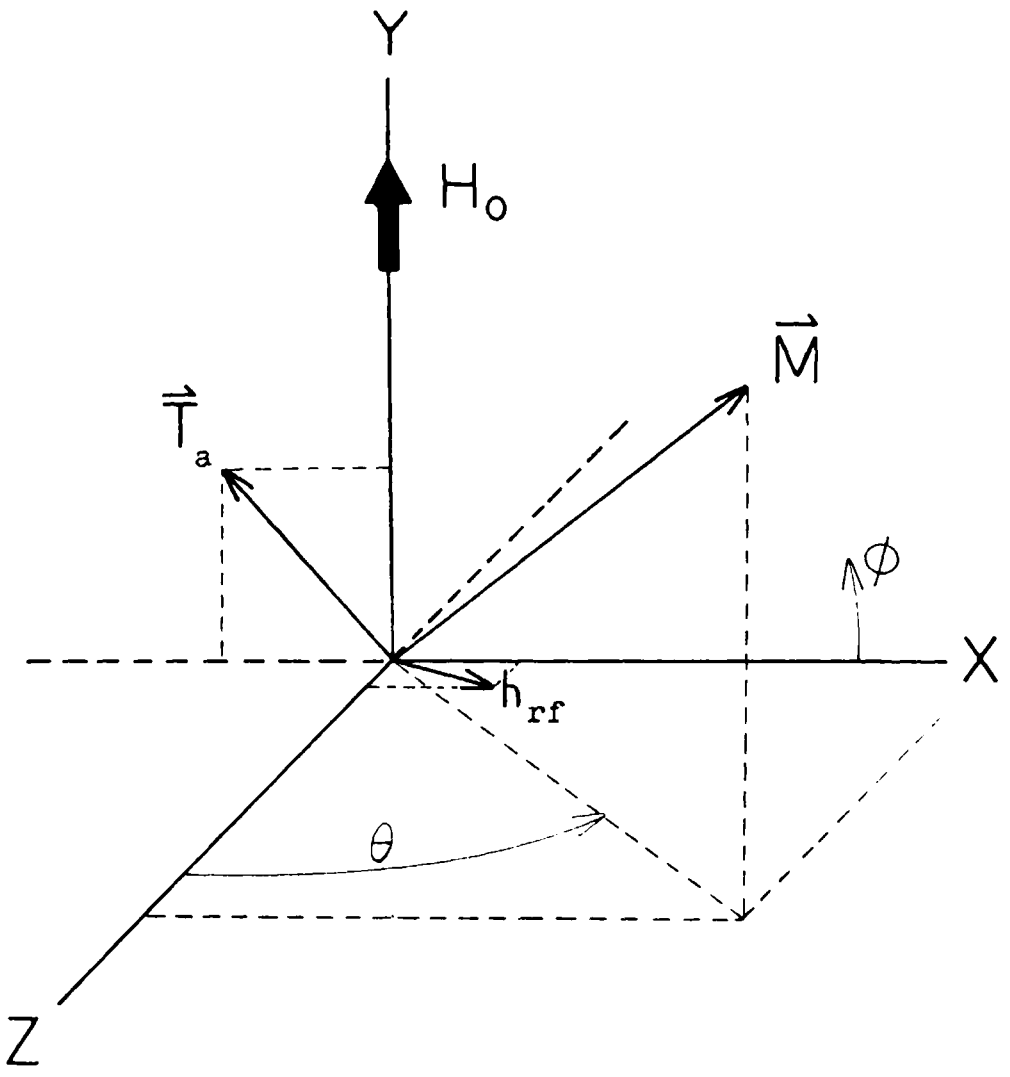


Figure 2.2 Orientation of Torque and Magnetization Vectors

$$\vec{T}_a = -2(K_1 + 2K_2) \frac{M_z}{M_s} \vec{a}_t \qquad (4)$$

Also at $\Theta = \frac{\pi}{2}$, Smit and Wijn (4) have defined the anisotropy field, $H_a$, to be:

$$H_a = \frac{-2(K_1 + 2K_2)}{M_s} \qquad (5)$$

The unit vector $\vec{a}_t$ for $\Theta \approx \frac{\pi}{2}$ can also be expressed in terms of the magnetization vector. From Figure 2.2 it can be seen that $\vec{a}_t = \sin \phi \, \vec{a}_x + \cos \phi \, \vec{a}_y$. The valid approximations for $\Theta \approx \frac{\pi}{2}$ are therefore $\sin \phi \approx \frac{M_y}{M_s}$ and $\cos \phi \approx \frac{M_x}{M_s}$. Substituting (5) into (4) and using the above approximations gives the desired form of the torque. This is:

$$\vec{T}_a = H_a M_z \left(-\frac{M_y}{M_s} \vec{a}_x + \frac{M_x}{M_s} \vec{a}_y\right) \qquad (6)$$

Consider now a magnetostatic field, sufficient for resonance, to be applied along the Y axis and the microwave field to be applied in the XZ plane. This is illustrated in Figure 2.2 and is the case of interest in this thesis. $\vec{M}$ and $\vec{H}_t$ can now be written as:

$$\vec{M} = m_x \vec{a}_x + M_s \vec{a}_y + m_z \vec{a}_z \qquad (7a)$$

$$\vec{H}_t = h_x \vec{a}_x + H_o \vec{a}_y + h_z \vec{a}_z \qquad (7b)$$

Substituting equations (6), (7a), and (7b) into the equation of motion yields the following simultaneous equations for an $e^{j\omega t}$ time dependence:

$$j\frac{\omega}{\gamma} m_x = M_s h_z - (H_o + H_a) m_z \tag{8a}$$

$$0 = h_x m_z - h_z m_x + H_a \frac{m_z m_x}{M_s} \tag{8b}$$

$$j\frac{\omega}{\gamma} m_z = m_x H_o - h_x M_s \tag{8c}$$

Assuming small signal operation, equation (8b) is eliminated from any further consideration as it is a second order equation in the small signal terms while (8a) and (8c) are first order. The simultaneous solution of equations (8a) and (8c) will yield the following in terms of $m_x$ and $m_z$:

$$m_x = \frac{M_s \left[ h_x(H_o + H_a) + j\frac{\omega}{\gamma} h_z \right]}{H_o (H_o + H_a) - (\frac{\omega}{\gamma})^2} \tag{9a}$$

$$m_z = \frac{M_s \left[ h_z H_o - j\frac{\omega}{\gamma} h_x \right]}{H_o (H_o + H_a) - (\frac{\omega}{\gamma})^2} \tag{9b}$$

Ignoring demagnetizing effects, the magnetic flux can be written as $\vec{b} = \vec{h} + 4\pi\vec{m}$ or $\vec{b} = (1 + [\overleftrightarrow{\chi}])\,\vec{h}$ where $\overleftrightarrow{\chi}$ is the susceptibility tensor determined from equations (9a) and (9b). In the present case, $\overleftrightarrow{\chi}$ can be written

$$\overleftrightarrow{\chi} = \begin{pmatrix} \chi_{xx} & 0 & -j\chi_{xz} \\ 0 & 1 & 0 \\ j\chi_{xz} & 0 & \chi_{zz} \end{pmatrix} \tag{10a}$$

where:

$$\chi_{xx} = \frac{4\pi M_s (H_o + H_a)}{H_o (H_o + H_a) - (\frac{\omega}{\gamma})^2} \tag{10b}$$

$$\chi_{zz} = \frac{4\pi M_s H_o}{H_o (H_o + H_a) - (\frac{\omega}{\gamma})^2} \tag{10c}$$

$$\chi_{xz} = \frac{4\pi M_s \frac{\omega}{\gamma}}{H_o (H_o + H_a) - (\frac{\omega}{\gamma})^2} \tag{10d}$$

The condition for resonance (1) is the singularity of this tensor, and is generally written as

$$(\frac{\omega}{\gamma})^2 = H_o (H_o + H_a) \tag{11}$$

An appropriate conversion factor applied to $\gamma$ results in an alternate form

$$(\frac{f}{\gamma})^2 = H_o (H_o + H_a) \tag{12}$$

The unit of $\gamma$ is megacycles per gauss if the conversion factor is $(2\pi \times 10^{+6})^{-1}$. The units of $\vec{M}$ and $\vec{H}$ are unchanged.

## 2.3 Damping

Losses were ignored in the preceding section on the derivation of the basic resonance equation. This can not be the true case. Damping, or losses, are always present but are not yet fully understood. There are two forms of damping terms that are added as torques in the equation of motion. These are the Landau-Lifschitz and the Bloch-Bloembergen terms (1). Damping processes will not be

considered in this thesis; therefore, only the general equation of motion for each damping formulation is given. These are (7),

Landau-Lifschitz

$$\frac{1}{\gamma}\frac{d\vec{M}}{dt} = \vec{M} \times \vec{H}_t + \vec{T}_a + \alpha \frac{\vec{M} \times (\vec{M} \times \vec{H}_t)}{\vec{M}} \qquad (13)$$

Bloch-Bloembergen

$$\frac{d M_{xy}}{dt} = \gamma (M \times H)_{xy} + \gamma (T_e)_{xy} - \frac{M_{xy}}{T_2} \qquad (14)$$

In (13), $\alpha$ is an experimentally determined constant while $T_2$ of (14) is a characteristic transverse relaxation time. The results caused by the introduction of these loss terms have been previously determined for a sphere. The Landau-Lifschitz formulation predicts a line width variation as a function of frequency while the Bloch-Bloembergen formulation predicts no frequency dependence of line width (7).

## 2.4 Demagnetization Effects

Had demagnetization effects been considered in the derivation of the resonance equation, the following equation would result (5):

$$\left(\frac{\omega}{\gamma}\right)^2 = \left[H_o - (N_x - N_y)\, 4\pi M_s\right]\left[H_o + H_a + (N_y - N_x) 4\pi M_s\right] \qquad (15)$$

The demagnetizing factors $N_x$, $N_y$, and $N_z$ are functions of the specimen geometry. Osborn derived these in 1945 for the general ellipsoid (1).

For spheres, the demagnetization factor in cartesian coordinates are equal and (15) yields (11) directly. Perfect spheres were not possible and eccentricity should be initially considered. The largest eccentricity of the two spheres occurred with $Zn_2Y$. Osborn's charts (1) were consulted and it was found that this eccentricity resulted in a three percent change in each demagnetization factor under the worst possible conditions of crystal orientation.

## 2.5 Spin Waves

A detailed analysis of spin waves is not considered in this thesis. However, an excellent general report on spin wave theory in the analysis of ferromagnetic resonance is made by Buffler (9).

In any resonance experiment a determination of the location within the finite sample manifold should be made (9). This will serve as an aid in evaluating experimental results. This determination was made using the known constants of $Zn_2Y$. These calculations, using $Ho = \frac{4\pi M_s}{3}$ and $Ho = \frac{8\pi M_s}{3}$, indicate that the "medium K state," or "no exchange region" of the spin wave manifold essentially covers the entire X-band. The assumption of only a uniform mode is valid in this region provided the sample diameter

is small compared with the microwave wave length. The largest diameter was .055 inches for $Mn_{0.5}Zn_{1.5}Y$ and for X-band the assumption is valid.

It is expected that line widths should broaden at each end of X-band. The broadening at the lower end of the band is due to domain formation as the sample unsaturates. At the upper end of the band the broadening is due to the coupling of the uniform mode to spin wave modes. The remaining portion in X-band should have a fairly constant line width (9).

# CHAPTER III

# EXPERIMENT

## 3.1 Sample Preparation and Mounting

Raw crystals of each compound were ground into small spheres utilizing a procedure and apparatus described by Stinson (10). It was found necessary to rough grind many $Zn_2Y$ crystals as they had imperfections that were not noticeable before grinding. The polished crystals to be used were selected for their nearness to spherical shape and for their uniformity of surface finish. The $Zn_2Y$ crystal selected was .015 inches in diameter and the $Mn_{0.5}Zn_{1.5}Y$ crystal was .055 inches in diameter. Both crystals had a uniform 600 grit finish.

Crystal orientation and mounting was accomplished with a small magnet. This magnet automatically oriented the sphere such that the basal plane of the crystal was perpendicular to the magnet surface. A wooden rod, tipped with Duco cement, was then lowered perpendicularly toward the magnet surface until the rod made contact with the ferrite. The glue was allowed to set before the ferrite was removed from the magnet. The wooden mounting rods were then cut to the desired length.

## 3.2 Experimental Equipment

Figure 3.1 is a block diagram of the X-band experimental arrangement that was used. All items are standard equipment with the exception of the modified coupler. The theory and operation of this coupler has been covered by others (7, 10, 11) and only a brief explanation of the additional modification will be given. This additional modification was necessary in that known angular variations of the sample within the coupler were desired. Basically this modification consists of a fixed reference disc, indexed at each ten degrees of arc; a movable indicator, indexed at each end; and an access hole for sample insertion. Figure 3.2 is a top view of the modified coupler in unassembled form. This permits the pertinent details of the movable indicator to be shown. These are the slit, hole, and adjusting bolts and are those items that give the vise type grip used to hold the wooden specimen rods. A completed assembly of the coupler is obtained by inserting a specimen rod (mounted on the movable indicator) into the access hole of the brass waveguide cap plug.

## 3.3 Measurements

Preliminary circuit tuning and line width measurements were made by following a procedure described by Stinson (10). Very simply, the peak value and the three

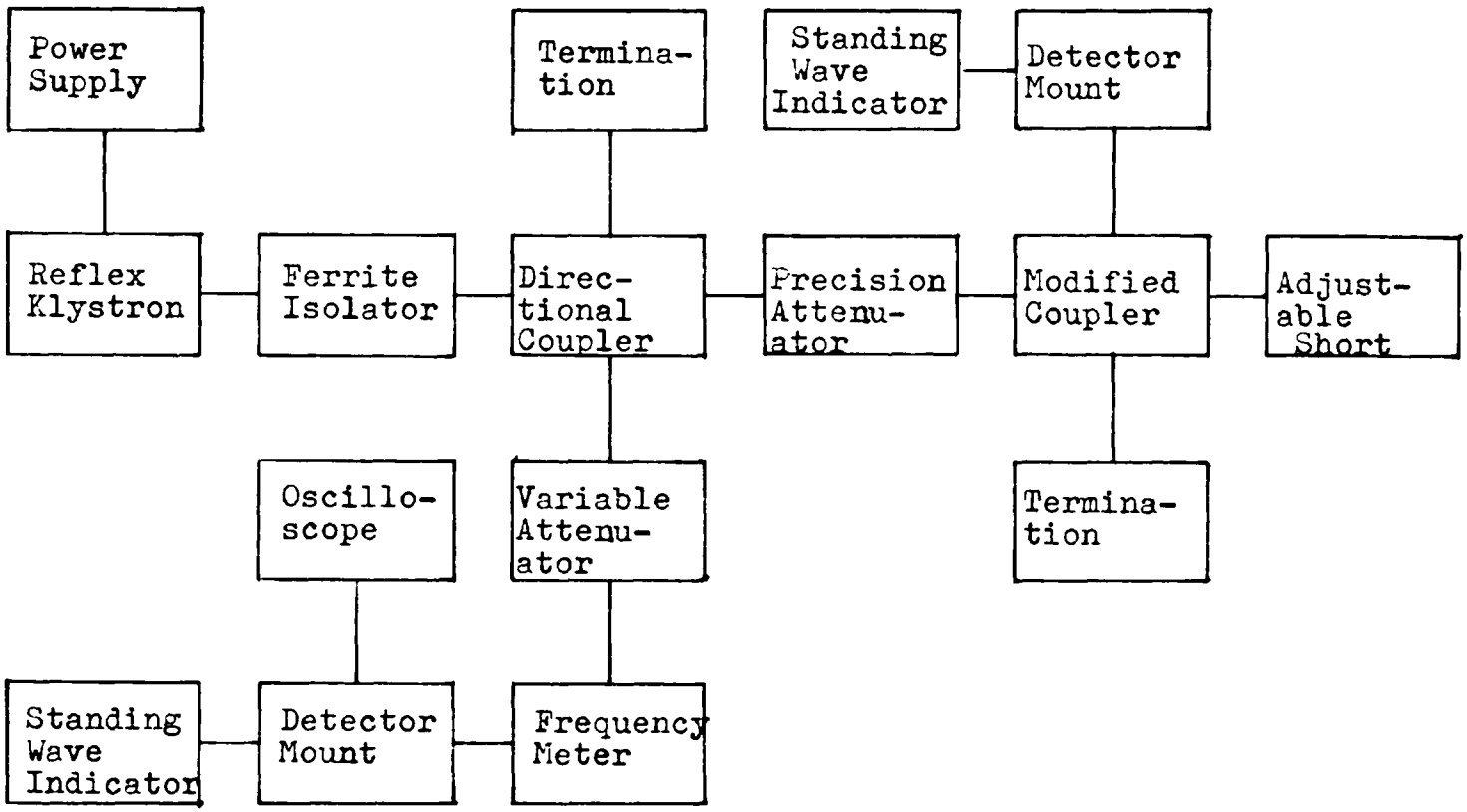


Figure 3.1 Block Diagram of Experimental Arrangement

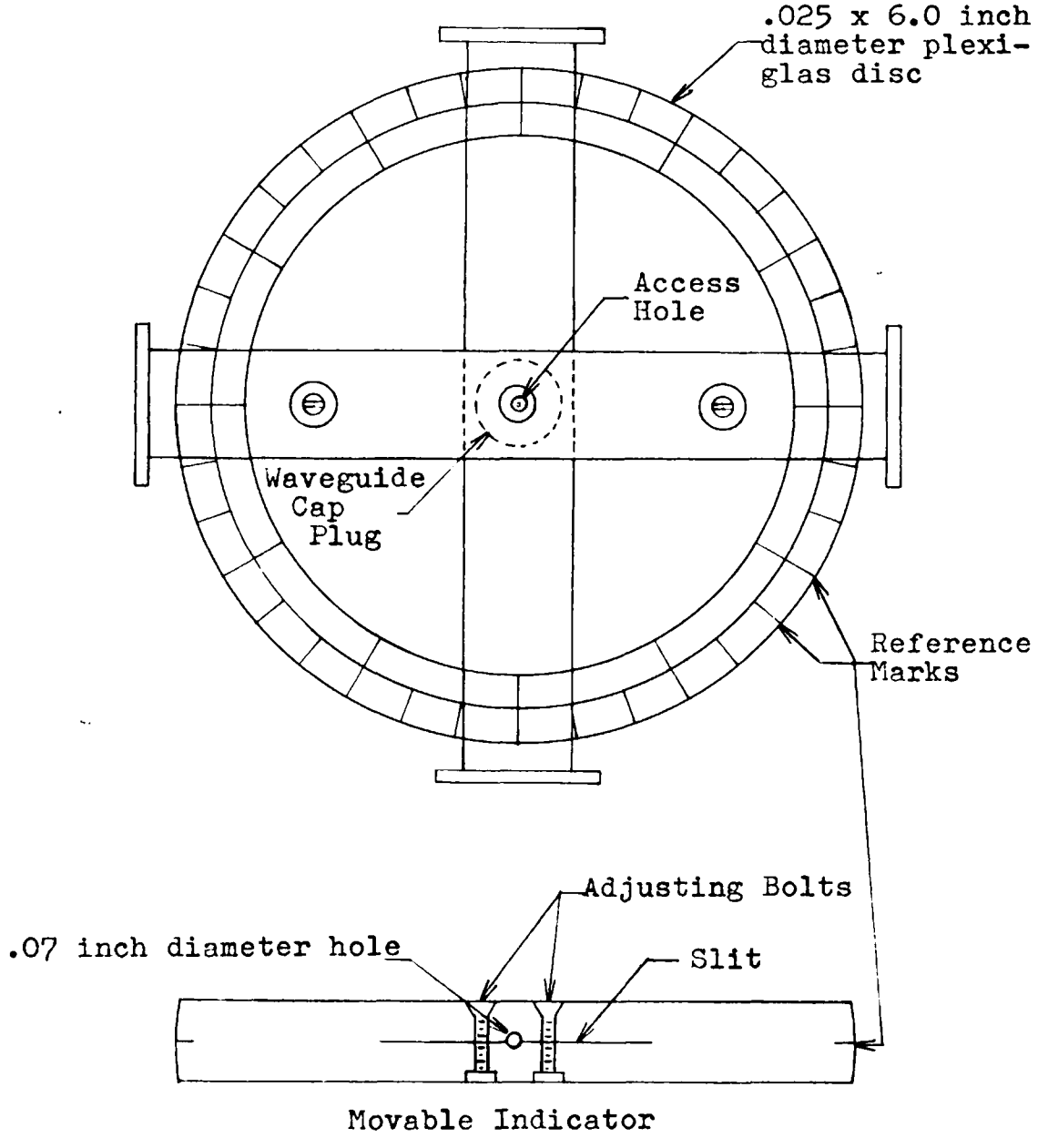


Figure 3.2 Top View of Modified Coupler

db points of the magnetostatic field resonance curve are measured. These values of magnetostatic field strength are determined from a precision guass meter. Nelson (12) describes the measurement technique and the additional equipment employed. There was only one variation from Nelson's procedure in that a Monroe calculator was used to determine field strengths from the guass meter oscillator frequency. This variation eliminated the interpolation of guass meter reading conversion tables that was required in the original method.

Each crystal was rotated through 180° in 20° increments at several X-band frequencies. This rotation was used to establish any possible symmetric behavior of the quantities in question. After several of these type measurements, the line widths with $h_{rf}$ perpendicular and $h_{rf}$ parallel to the basal plane were measured for a variety of frequencies in X-band.

## 3.4 Experimental Results

For the discussion of all experimental results and for all graphs that follow, 0° is used to reference $h_{rf}$ parallel to the basal plane. The angle between $h_{rf}$ and the basal plane will arbitrarily be called theta and is not to be confused with the usual theta that is used in spherical coordinates.

The results of angular rotation of $Zn_2Y$ for 8.6gc and 9.0gc are given in Figure 3.3. These frequencies were selected as being representative of the other frequencies checked. A general angular dependence of the line width appeared to be $\sin^2\theta$, while the resonant magnetostatic field was too irregular to warrant any such simple angular description. A reversal of line width is quite apparent in these graphs. The actual reversal occurred in the vicinity of 8.7gc. This can be seen quite easily in Figure 3.4 where line width at angles of 0° and 90° are plotted versus frequency. This anomalous reversal of line width can be explained by theory in conjunction with the resonant magnetostatic field angular variation.

The basic resonance equation does not predict an angular dependence for the resonant magnetostatic field. Nevertheless, this field was angular dependent even though no simple angular description existed. At all frequencies, the resonant magnetostatic field was a minimum at 0° and a maximum at 90°. This behavior can be accounted for in theory by anisotropic g factors (9). These anisotropic g factors will also directly affect the critical frequencies mentioned in Chapter II. In this case, the critical frequencies at 0° are higher and unsaturation will start sooner. This effect has been large enough to give the line width reversal at 8.7gc.

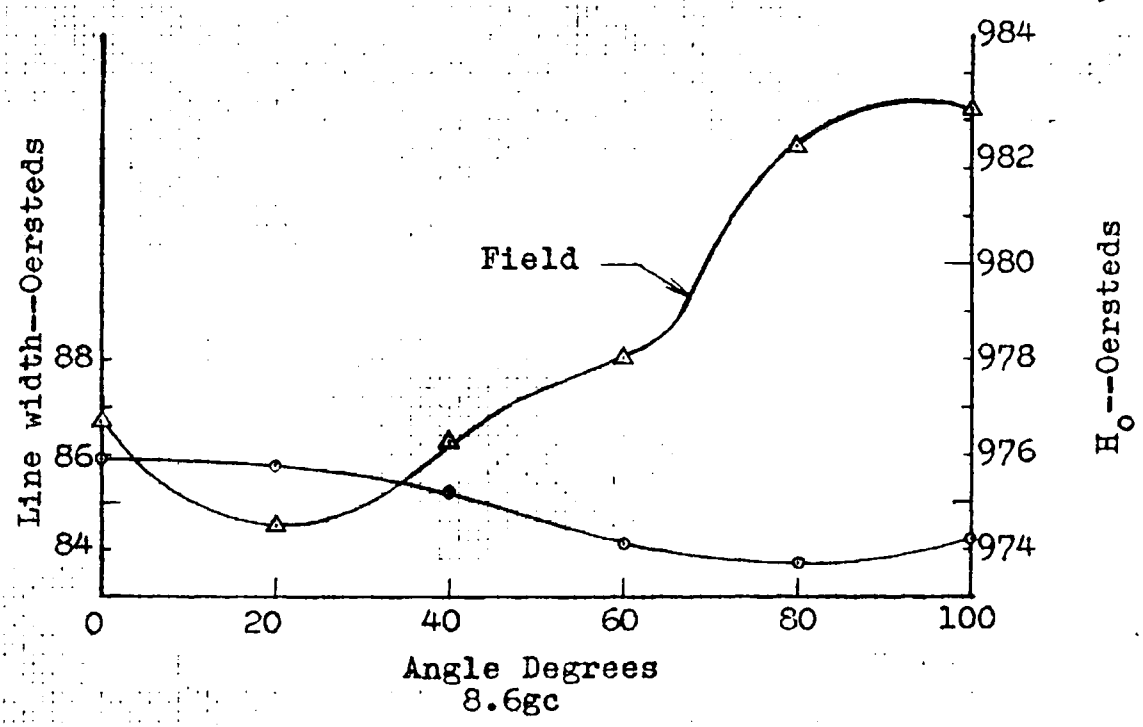


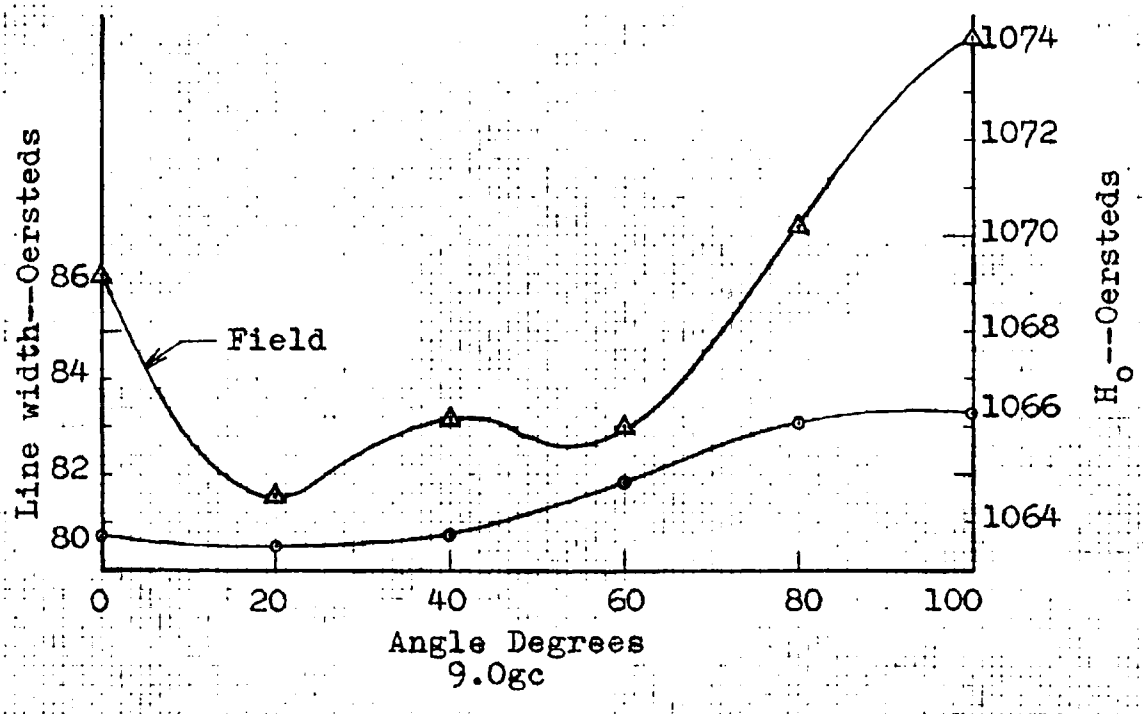


Figure 3.3 Graphs of Magnetostatic Field and Line Width versus Angle for $Zn_2Y$

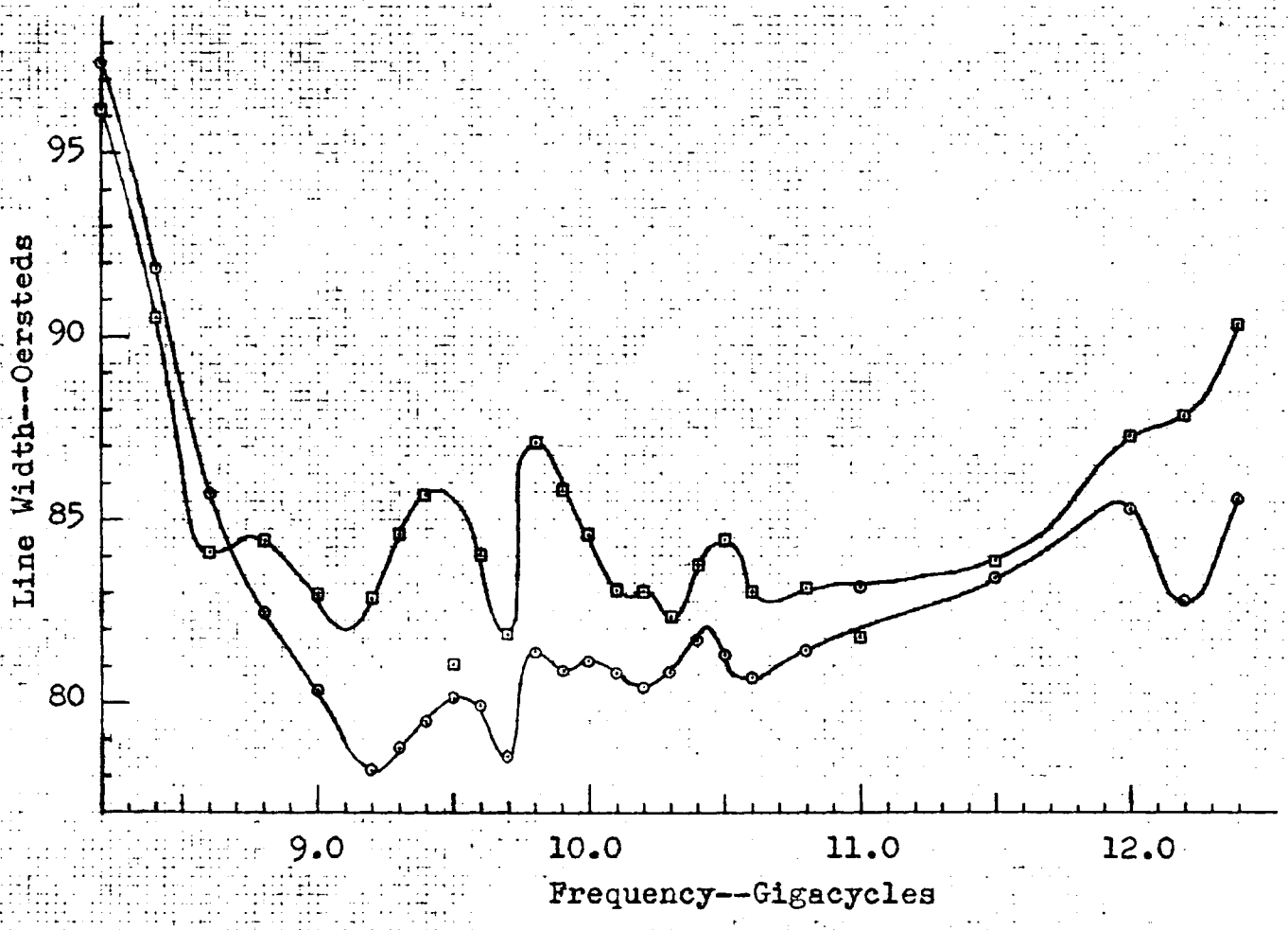


Figure 3.4 Graph of Line Widths versus Frequency for $Zn_2Y$

The gross behavior of line width versus frequency in Figure 3.4 also agrees with theory which predicts that compounds having negative anisotropy constants will have increasing line widths with increasing frequency (4, 9). This behavior is somewhat masked as line width broadening was anticipated due to the uniform mode coupling to spin waves at the upper end of X-band.

Figure 3.5 is a plot of the magnetostatic field versus frequency with hrf applied in the basal plane. A best fit was made to this data yielding $H_\theta$ = 9875 oersted and $\gamma' = 2.62$. These results are in excellent agreement with Buffler (5) who obtained $H_\theta$ = 9900 oested and $\gamma' = 2.62$.

The results of angular rotation of $Mn_{0.5}Zn_{1.5}Y$ at 8.4gc and 9.4gc are given in Figure 3.6. As with $Zn_2Y$, these frequencies were considered representative of the other frequencies. The line width curves have a good $\sin^2\theta$ variation as did those for $Zn_2Y$. However, the resonant magnetostatic field is essentially a constant in contrast to the irregular behavior noted for $Zn_2Y$.

The frequency behavior of the line widths (Figure 3.7) and of the magnetostatic field (Figure 3.8) were much smoother and in better agreement with theory than the similar plots for $Zn_2Y$. The line width pattern of Figure 3.7 also infers a smaller anisotropy field and saturation magnetization in that the line widths have not broadened at the low end of X-band. The peak at 12.0gc may not be

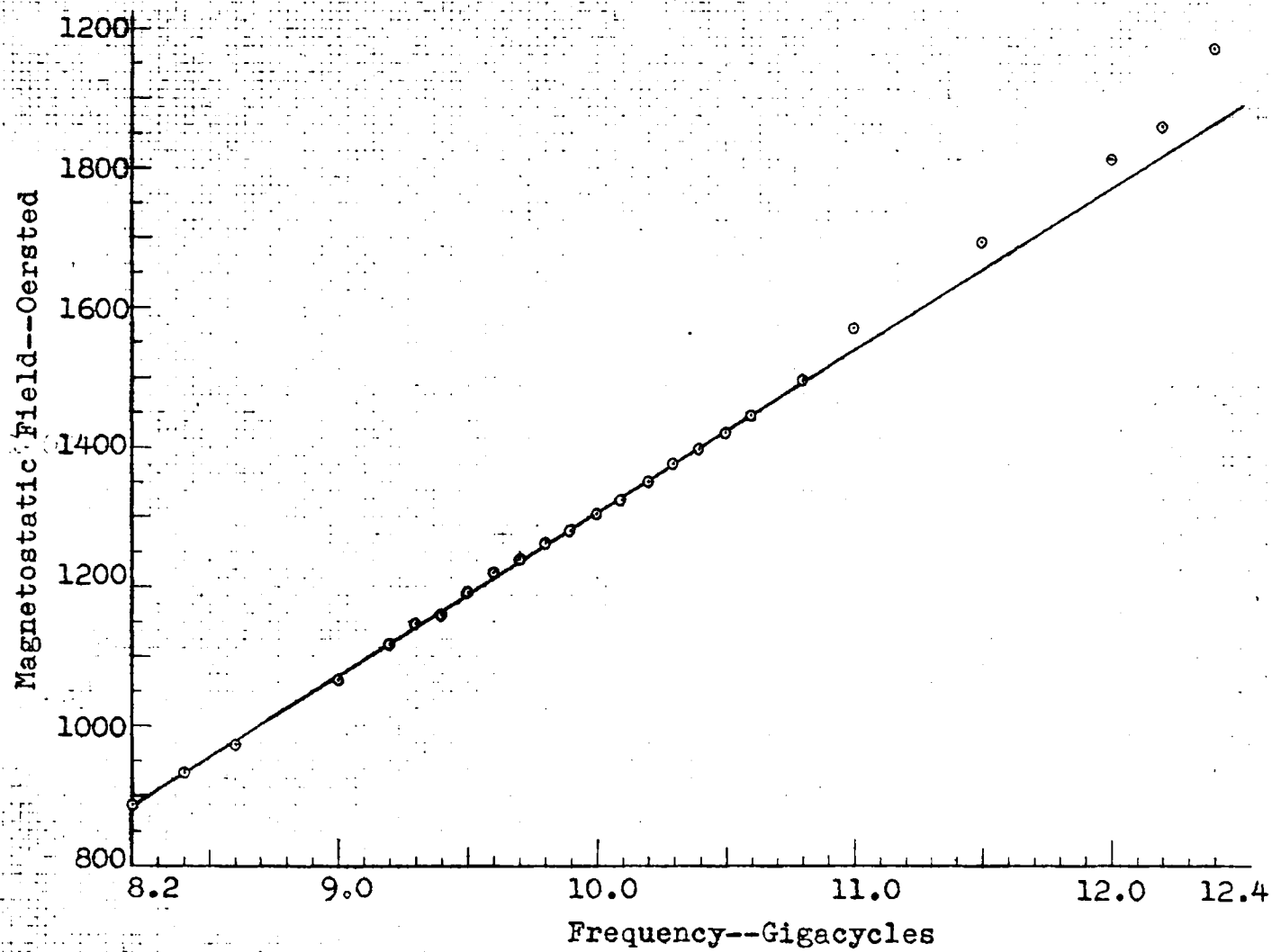


Figure 3.5 Graph of Resonant Magnetostatic Field versus Frequency for $Zn_2Y$

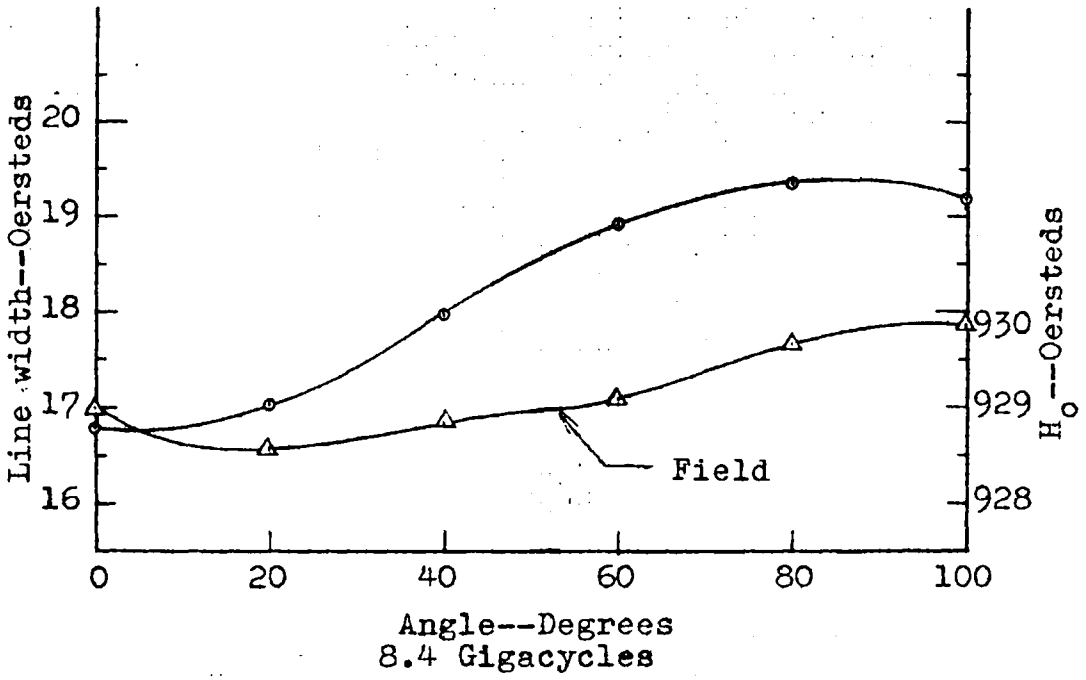


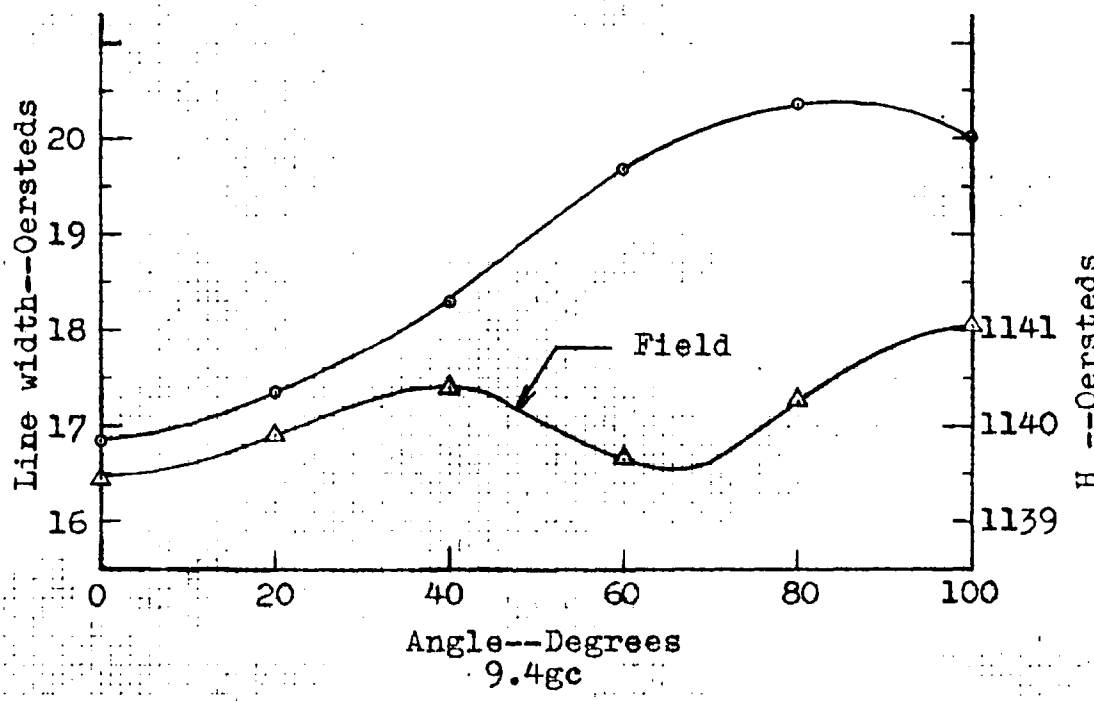


Figure 3.6 Graphs of Magnetostatic Field and Line Width versus Angle for $Mn_{0.5}Zn_{1.5}Y$

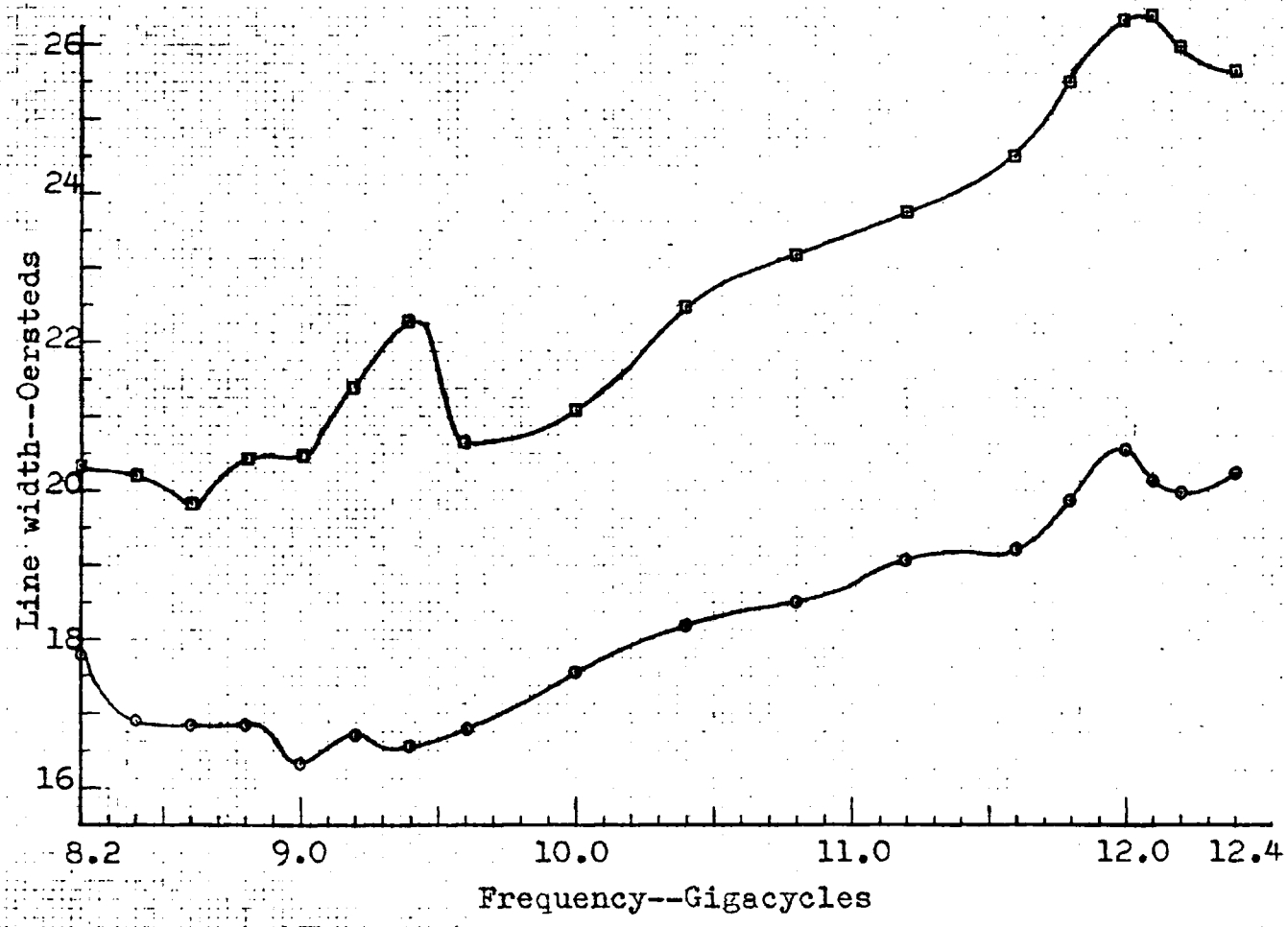


Figure 3.7 Graph of Line Widths versus Frequency for $Mn_{0.5}Zn_{1.5}Y$

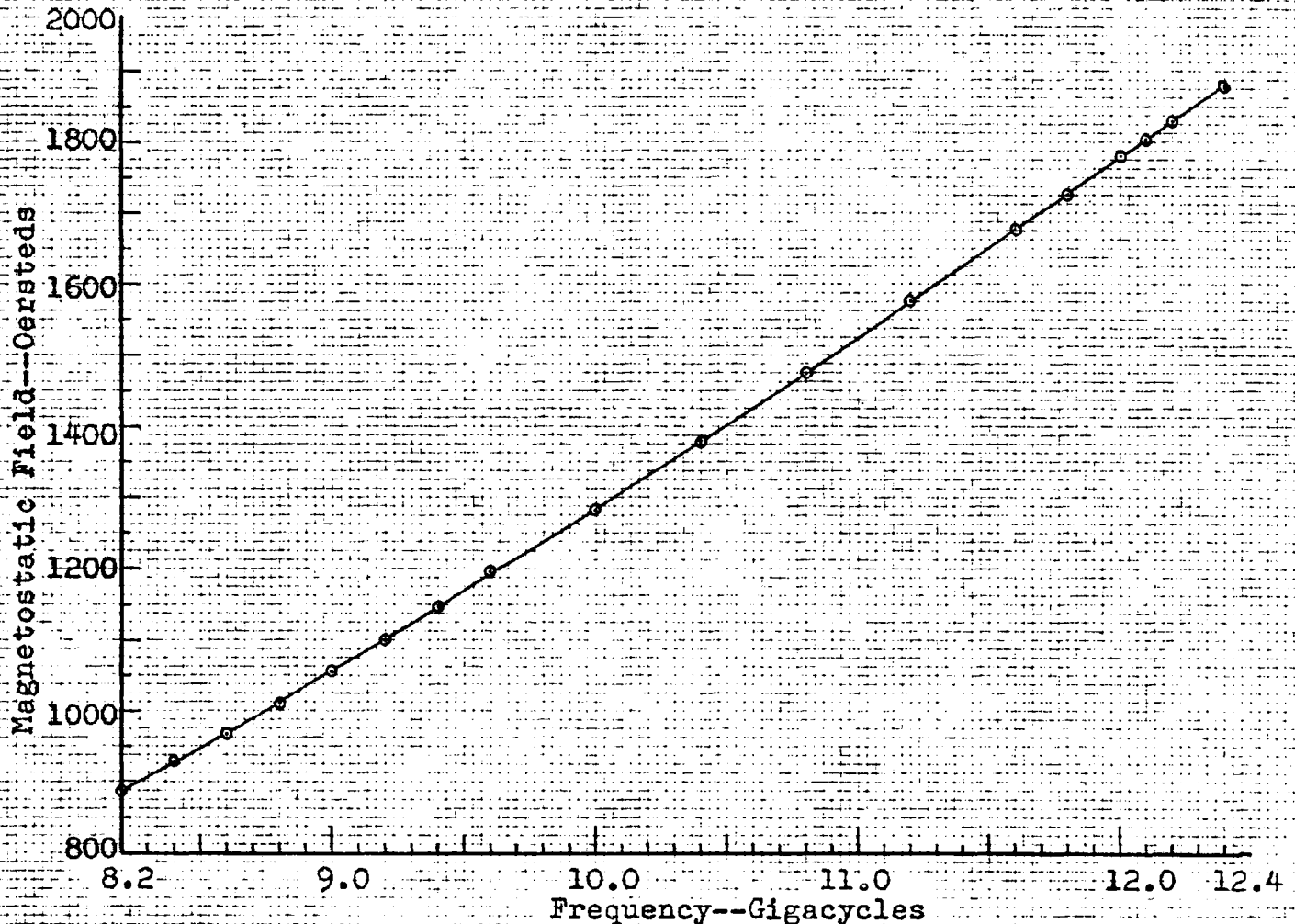


Figure 3.8 Graph of Resonant Magnetostatic Field versus Frequency for $Mn_{0.5}Zn_{1.5}Y$

the peak expected at the high end of X-band because it is much smaller than anticipated (9).

A best fit of the data from the resonant magnetostatic field versus frequency (Figure 3.8) was made to determine $H_\Theta$ and $\gamma'$. This resulted in $H_\Theta$ = 9560 oersted and $\gamma'$ = 2.69 mc/gauss.

It was found during the course of the experiment that the 3db points of the resonance curve for $Zn_2Y$ had a better angular correspondence with line width than did the measured resonant magnetostatic field. At first it was thought that a more accurate determination of the resonant magnetostatic field might be made by averaging the two 3db points which had implied a symmetric resonance curve. However, shape anisotropy had been neglected and the angular sensitivity of the anisotropic g factor was not known. These two factors can account for variations of the peak value in the resonance curve and not cause any variation in the two 3db points (9). Therefore, any inference using the 3db points was not made.

The behavior of the two 3db points was also checked for $Mn_{0.5}Zn_{1.5}Y$. In this compound the behavior was entirely different from that observed in $Zn_2Y$. The upper 3db point followed the line width variation and the lower 3db point was constant. This behavior also implied the possibility of a constant (with angle) resonant

magnetostatic field. This was verified by other experimental results.

Power sensitivity and angular dependence of the coupled power for both ferrites was also observed during the experiment, however, no investigation was made into these characteristics.

# CHAPTER IV

# CONCLUSIONS

## 4.1 Conclusions

The following facts are concluded from the experimental results:

1. Angular dependence of line widths is a sine squared of the angle variation for both compounds.
2. The resonant magnetostatic field for $Mn_{0.5}Zn_{1.5}Y$ has no angular variation.
3. The angular variation of the resonant magnetostatic field for $Zn_2Y$ is attributed to anisotropic g factors.
4. The crossguide coupler technique allows accurate determination of resonance equation parameters.

## 4.2 Recommendations for Future Study

1. A study of the different shapes of the magnetostatic resonance curves for $Zn_2Y$ and $Mn_{0.5}Zn_{1.5}Y$ should be made.
2. The effects of the large magnetocrystalline field on the resonance equation parameters and line width for other crystal orientations should be investigated.

3. The angular dependence of coupled power should be studied.

## LIST OF REFERENCES


1. Lax, B. and K. J. Button, Microwave Ferrites and Ferrimagnetics, New York: McGraw-Hill, Inc., 1962.

2. Neel, L., "Proprietes magnetiques des ferrites, ferrimagnetisme et antiferromagnetisme," Ann. Phys., Vol. 13, 1948, p. 137.

3. Shaw, H. J., "Pulsed Magnetic Field Millimeter Wave Generator," Microwave Laboratory, Stanford Univ., 1962.

4. Smit, J. and H. P. J. Wijn, Ferrites, John Wiley and Sons, Inc., 1959.

5. Buffler, C. R., "Resonance properties of single crystal hexagonal ferrites," J. Appl. Phys., Vol. 33, March 1962, p. 1360.

6. Tauber, A., private communication

7. Bowers, R. K. and D. C. Stinson, "The frequency dependence of the line width of polycrystalline yttrium garnet ferrites," Eng. Exp. Sta. Bul. No. 12, EE Ser No. 3, July 1960.

8. Bady, I., "Ferrites with planar anisotropy at microwave frequencies," IRE Trans of Microwave Theory and Techniques, Vol. MTT-9, January 1961.

9. Buffler, C., "A Spin Wave Analysis of Ferromagnetic Resonance Relaxation," Gordon McKay Laboratory of Applied Science, Harvard Univ., February 1960.

10. Stinson, D. C., "Ferrite line width measurements," Paper No. CP 61-1005, University of Arizona, August 1961.

11. Stinson, D. C., "Ferrite line width measurements in a cross-guide coupler," IRE Trans on Microwave Theory and Techniques, Vol. MTTT-6, October 1958.

12. Nelson, T. C., "Angular dependence of the line width of a planar ferrite," Thesis, University of Arizona, 1963.